Comparison of Switching Phenomena in Chaotic Maps or a Chaotic Circuit

Tomoko Yamada
Dept. Information Science,
Shikoku University
Email: s1839074@keiei.shikoku-u.ac.jp

Yasuteru Hosokawa
Dept. Information Science,
Shikoku University
Email: hosokawa@keiei.shikoku-u.ac.jp

Yoshifumi Nishio
Dept. Electrical and Electronic Eng.,
Tokushima University
Email: nishio@ee.tokushima-u.ac.jp

***Summary*— Some chaotic systems have two coexisting attractors depending on initial values in same parameters. In these systems, changing parameters causes switching phenomena of coexisting attractors. In this study, we investigate switching phenomena of coexisting attractors in one-dimensional maps or a chaotic circuit. The purpose of this study is to compare a element of CML with a element of coupled chaotic circuits. By using results of this study, we will investigate the relationship between CML and coupled chaotic circuits.**

I. Introduction

Some chaotic systems have two coexisting attractors depending on initial values in same parameters [1]-[3]. In these systems, changing parameters causes switching phenomena of coexisting attractors. We consider that matching two attractors in coupled systems which have two coexisting attractors means the phenomenon like a very weak synchronization. By investigating switching phenomena in the system, it is expected that some interesting phenomena are observed in coupled systems which have two coexistence attractors.

In this study, we investigate switching phenomena in one-dimensional maps and a chaotic circuit. The chaotic circuit is Shinriki-Mori circuit [1][2]. The purpose of this study is the comparison between chaotic elements of CML [4] and coupled chaotic circuits. Namely, results of this study can make a contribution to the comparison between CML and coupled chaotic circuits.

II. System Models

A. Chaotic Map

In order to investigate switching phenomena, two kinds of one-dimensional maps are investigated in this study. The functions of two maps are shown as follows.

$$x_{n+1} = -ax_n^3 + ax_n. \tag{1}$$

$$x_{n+1} = -ax_n + a|x_n + \frac{1}{2}| - a|x_n - \frac{1}{2}|. \tag{2}$$

Figures 1 and 2 show the one-dimensional maps derived by Eqs. (1) and (2), respectively. Two coexisting attractors are observed (red and blue.) Same parameters and different initial values are used in Figs. 1 (a) and 1 (b) and Figs. 2 (a) and 2 (b), respectively. By increasing a, switching phenomena are observed in Figs. 1 (c) and 2 (c). These are symmetric about the origin.

Figures 3 and 4 show one parameter bifurcation diagrams of Eq. (1) and Eq. (2), respectively. Switching phenomena are observed between $2.60 < a < 3.00$ and $2.00 < a < 3.00$. In Fig. (1), period doubling phenomena are observed. In Fig. (2), chaotic phenomena are observed in $1.00 < a < 3.00$. In order to investigate switching phenomena, we define region D^+ and D^- as right and left side attractors of Figs. 1 and 2. Transitional conditions are shown as follows.

$$\begin{aligned} D^+ &\rightarrow D^-\text{: when } x > 0 \text{ and becomes } x < 0. \\ D^- &\rightarrow D^+\text{: when } x < 0 \text{ and becomes } x > 0. \end{aligned} \tag{3}$$

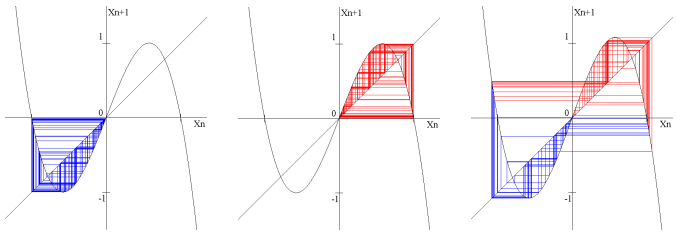

Fig. 1. The one-dimensional maps described by Eq. (1). (a) $a = 2.6$ and $x_0 = -0.4$. (b) $a = 2.6$ and $x_0 = 0.4$. (c) $a = 2.8$ and $x_0 = 0.4$.

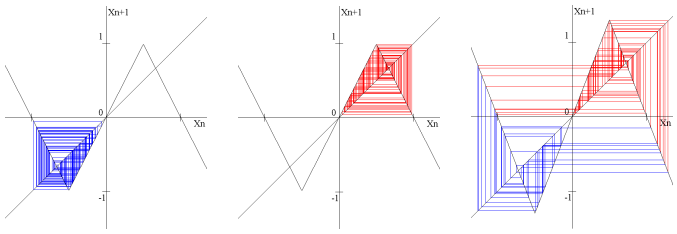

Fig. 2. The one-dimensional maps described by Eq. (2). (a)$a = 1.97$. and $x_0 = -0.40$. (b)$a = 1.97$. and $x_0 = 0.40$. (c)$a = 2.60$. and $x_0 = 0.40$

B. Chaotic Circuit

Figure 5 shows the chaotic circuit used in this study. The circuit equation is described as follows.

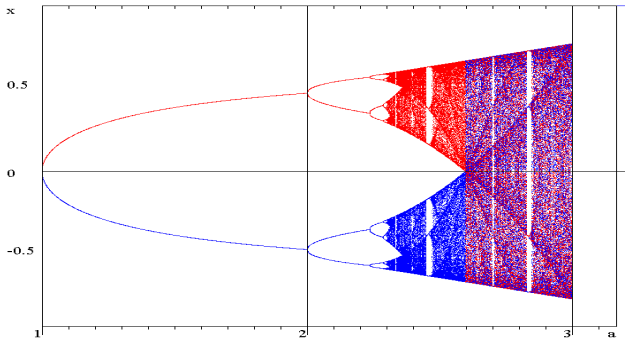

Fig. 3. The one parameter bifurcation diagram of Eq. (1). $1 < a < 3$. Red: the initial value of x is 0.4. Blue: the initial value of x is -0.4.

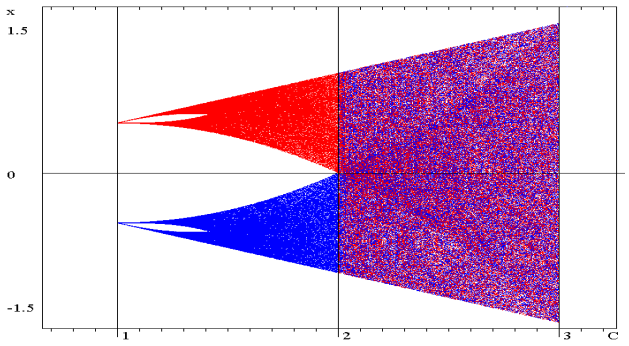

Fig. 4. The one parameter bifurcation diagram of Eq. (2). $a = -2.75$ and $1 < c < 3$. Red: the initial value of x is 0.4. Blue: the initial value of x is -0.4.

$$\begin{cases} L\dfrac{di}{dt} &= v_1, \\ C\dfrac{dv_1}{dt} &= -i - i_d, \\ C_0\dfrac{dv_2}{dt} &= gv_2 + i_d, \end{cases} \tag{4}$$

where,

$$i_d = \begin{cases} a(v_1 - v_2 - V_{th}), & v_1 - v_2 > V_{th}, \\ 0, & -V_{th} \le v_1 - v_2 \le V_{th}, \\ a(v_1 - v_2 + V_{th}), & v_1 - v_2 < -V_{th}. \end{cases} \tag{5}$$

Two diodes are modeled as a piece-wise linear function shown in Fig. 6.

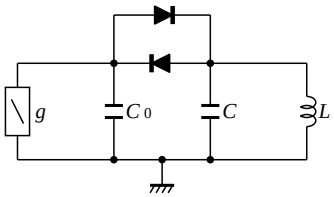

Fig. 5. Shinriki-Mori chaotic circuit.

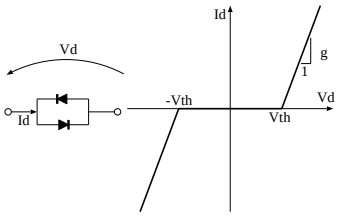

Fig. 6. Diodes model.

Changing variables and parameters as follows,

$$\begin{aligned} &x = \frac{1}{V_{th}}\sqrt{\frac{L}{C}}\cdot i, \quad y = \frac{1}{V_{th}}\cdot v_1, \quad z = \frac{1}{V_{th}}\cdot v_2 \\ &\alpha = a\sqrt{\frac{L}{C}}, \quad \beta = g\frac{C}{C_0}\sqrt{\frac{L}{C}}, \quad \gamma = \frac{C}{C_0}, \\ &\tau = \frac{1}{\sqrt{LC}}t, \quad \frac{d}{d\tau} = \text{" }\cdot\text{ "} \end{aligned} \tag{6}$$

Normalized circuit equation is described as follows.

$$\begin{cases} \dot{x} = & y, \\ \dot{y} = & -x - f(y - z), \\ \dot{z} = & \beta z + \gamma f(y - z), \end{cases} \tag{7}$$

where,

$$f(y-z) = \begin{cases} \alpha(y - z - 1), & y - z > 1, \\ 0, & -1 \le y - z \le 1, \\ \alpha(y - z + 1), & y - z < -1. \end{cases} \tag{8}$$

Using this equation, computer simulations are carried out.

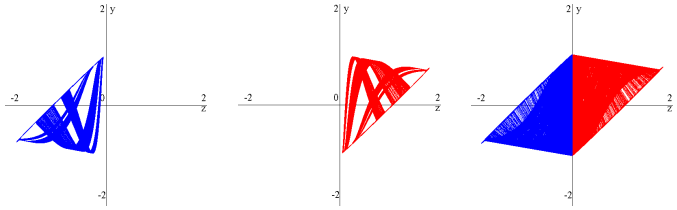

Fig. 7. Computer simulation results of the chaotic circuit. $\alpha = 10.0$ and $\gamma = 2.605$. (a) $\beta = 0.54$. (b) $\beta = 0.54$. (c) $\beta = 0.56$. Differential initial values are used in (a) and (b).

Figure 7 shows some computer simulation results. Horizontal axis is z. Vertical axis is y. Two attractors shown in Fig. 7 (a) and Fig. 7 (b) are observed in same parameters. Here, we define region D^+ and D^- as right and left side attractors of Fig. 7 respectively. Transitional conditions are shown as follows.

$$\begin{aligned} &D^+ \to D^-\text{: when } y - z > -1 \text{ and becomes } y - z < -1. \\ &D^- \to D^+\text{: when } y - z < 1 \text{ and becomes } y - z > 1. \end{aligned} \tag{9}$$

Increasing β, coexistence of attractors are observed shown as Fig. 7 (c). Figure 8 shows the one parameter bifurcation diagram of the chaotic circuit. The case that the initial value is 0.11 is shown as red. The case that the initial value is -0.11 is shown as blue. Switching phenomena are observed from $\beta = 0.56$ to $\beta = 0.68$.

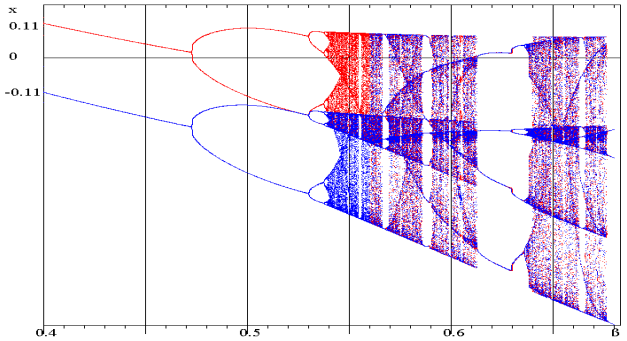

Fig. 8. The one parameter bifurcation diagram of the chaotic circuit. $\alpha = -2.75$ and $0.4 < \beta < 0.68$.

III. Switching Phenomena

A. Chaotic Map

Figure 9 shows the magnification of a third-order polynomial function as shown in Eq. (1). In the case of $1 < x < \frac{2\sqrt{3}}{9}a$, switching are occurred. In the case of $0 < x < 1$, switching are not occurred. In order to carry out the theoretical analysis, we assume that the distribution of x is homogeneous distribution. Using this assumption, we can described the switching rates SR_i as follows.

$$SR_i = \frac{3\sqrt{3}}{2a}. \tag{10}$$

In the case of Eq. (2), the switching rates SR_t can be also described as follows.

$$SR_t = \frac{2}{a}. \tag{11}$$

Figures 10 and 11 show relationships between parameter a and switching rates. Yellow lines show SR_i and SR_t, respectively. Blue and red lines show switching rates calculated by computer simulations. Blue and red lines are the same because this map is symmetric about the origin. Some local maximums are observed by periodic orbits called as a window. In the case of Fig. 10, switching rates differ from SR_i. We consider that the reason is the distribution of x is not homogeneous. However, these gradients are similar. In the case of Fig. 11, switching rates is very close with SR_t, because the distribution of x is similar to homogeneous.

B. Chaotic Circuit

Figure 12 shows the relationship between parameter β and switching rates of the chaotic circuit. Horizontal axis shows β and vertical axis shows switching rates. This system is not symmetric in the origin. Therefore, red and blue lines are not the same.

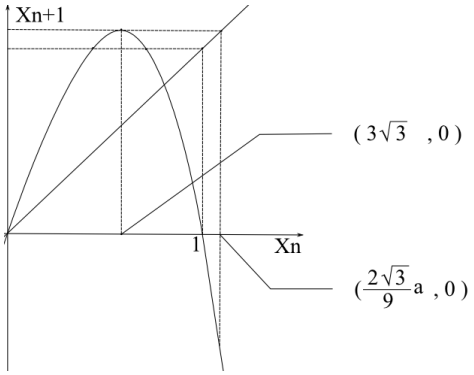

Fig. 9. The magnification of a third-order polynomial function.

C. Comparison

Major difference between the maps and the circuit is that chaotic maps are symmetry systems and the chaotic circuit is asymmetry system. However, increasing parameter a or β increase switching rates. These results show that these systems are similar. In the cases of Figs. 10 and 12, some peaks of rates are observed by windows. In the case of Fig. 11, any peak are not observed because there is no window as shown in Fig. 4.

As a result of this comparison, we can say that as follows.

- Eq. (1) and the chaotic circuit can observe similar phenomena.
- Switching rate of Eq. (1) is not much to Eq. (10).
- Switching rate of Eq. (2) is much to Eq. (11).

Therefore, in order to investigate coupling systems, Modifying Eq. (1) or detecting a chaotic circuit whose observed phenomena is similar to Eq. (2).

IV. Conclusions

We have investigated switching phenomena of coexisting attractors in two one-dimensional maps and a chaotic circuit. As a result, closing phenomena which is observed in chaotic maps and a circuit is needed in order to compare the chaotic map and the chaotic circuit. By closing observed phenomena, we will investigate the switching phenomena of CML and coupled chaotic circuits.

References

[1] M. Shinriki, M. Yamamoto and S. Mori, "Multi-mode Oscillations in a Modified van der Pol Oscillator Containing a Positive Nonlinear Conductance," *Proc. IEEE*, vol. 69, pp. 394-395, 1981.

[2] N. Inaba, T. Saito and S. Mori, "Chaotic Phenomena in a Circuit with a Negative Resistance and an Ideal Switch of Diodes," *Tran. IEICE*, vol. E70, no. 8, 1987.

[3] Y. Nishio, N. Inaba, S. Mori and T. Saito, "Rigorous Analyses of Windows in a Symmetric Circuit," *IEEE Tran. Circuits Syst.*, vol. 37, no. 4, 1990.

[4] K. Kaneko, "Spatiotemporal Intermittency in Coupled Map Lattices," *Prog. Theor. Phys.* vol. 74, no. 5, pp. 1033-1044, 1985.

[5] M. Wada, K. Kitatsuji and Y. Nishio, "Spatio-Temporal Phase Patterns in Coupled Chaotic Maps with Parameter Deviations," Proc. NOLTA'05, pp. 178-181, Oct. 2005.

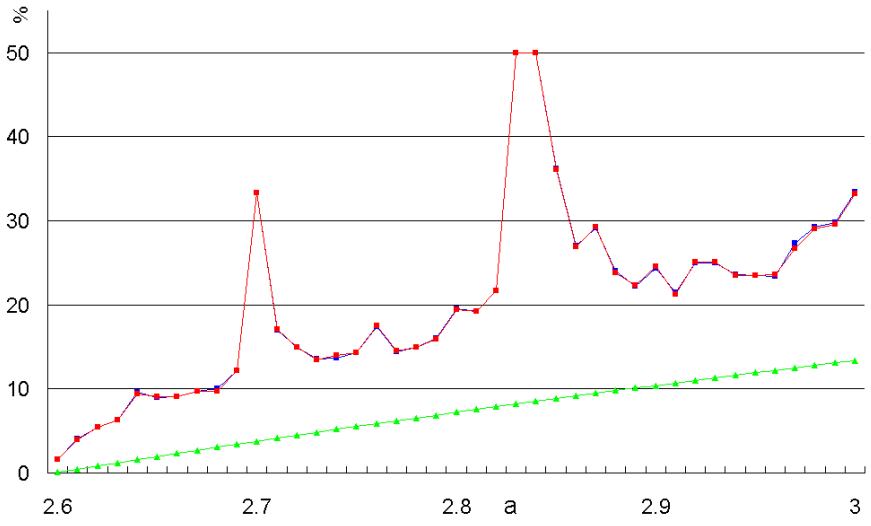

Fig. 10. Switching rates of the chaotic map described by Eq. (1). Red: $D^+ \to D^-$. Blue: $D^- \to D^+$. Green: Calculating results of Eq. (10).

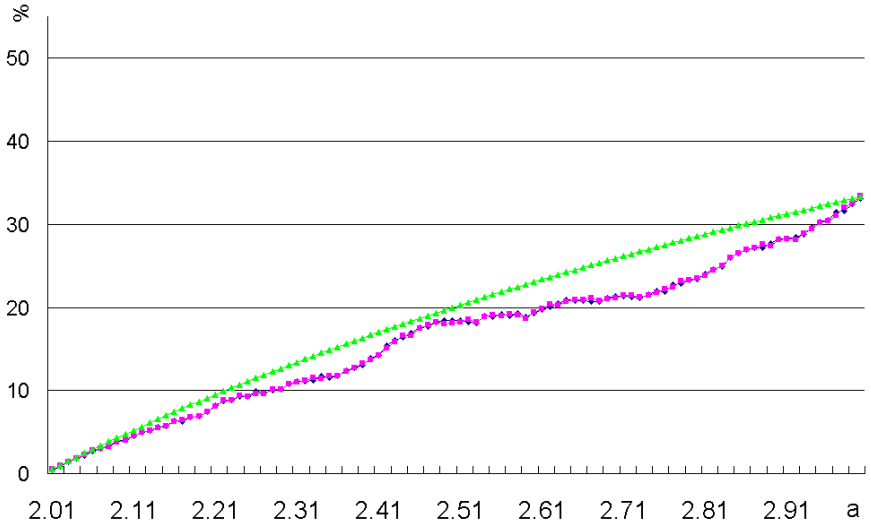

Fig. 11. Switching rates of the chaotic map described by Eq. (2). Red: $D^+ \to D^-$. Blue: $D^- \to D^+$. Green: Calculating results of Eq. (11).

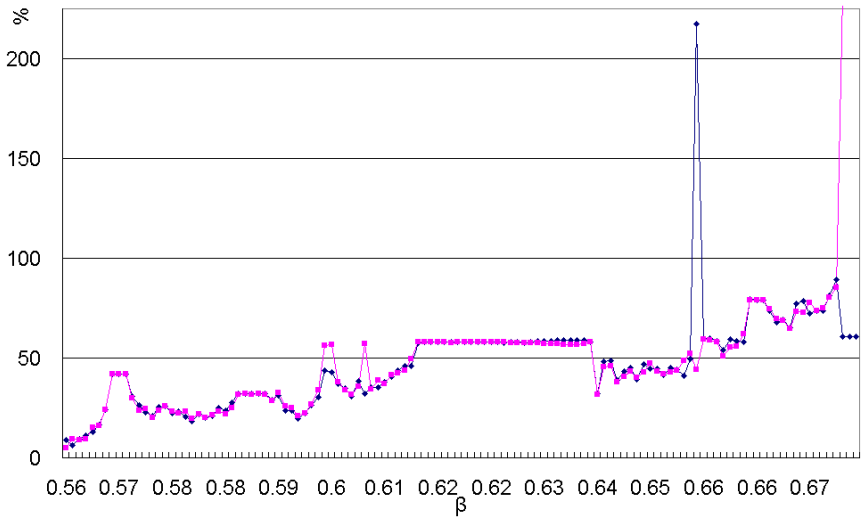

Fig. 12. Switching rates of the chaotic circuit. $\alpha = 10.0$, $\gamma = 2.605$ and $0.56 < \beta < 0.68$.